

5. K. A. Fuchs, Vaporization and Drop Growth in a Gas [Russian translation], Izd. Akad. Nauk SSSR, Moscow (1968).
6. M. V. Buikov and S. S. Dukhin, "Diffusional and thermal relaxation of vaporizing drops," *Inzh.-Fiz. Zh.*, No. 3, 80-87 (1962).
7. D. I. Polishchuk, "Vaporization of water drops at ambient temperatures above the boiling point," *Zh. Tekh. Fiz.*, 23, No. 12, 2151-2158 (1953).
8. H. B. Dwight, Tables of Integrals and Other Mathematical Data, Macmillan (1961).

MATHEMATICAL MODELING OF THE HEAT-TRANSFER  
PROCESS AND SOLID PARTICLES IN A FLUIDIZED BED

V. A. Borodulya, Yu. S. Teplitskii,  
Yu. G. Epanov, Yu. E. Livshits,  
and I. I. Yanovich

UDC 66.096.5

The authors formulate a two-concentration model of particle mixing in a fluidized bed, accounting for particle inertia.

In spite of the importance of knowing the laws for transfer of heat and particle mass in a fluidized bed, this matter has not yet been satisfactorily resolved. Existing methods account for some of the real transport properties of the system, but there is no model that describes at least the basic features of the bed and includes the present methods of describing the mixing phenomenon as special cases. For example, the simplest diffusion model [1] examines the particle transport process as a purely random diffusion one. The circulation mixing method [2] singles out convective particle transport as the basic mechanism (upwards in the trails of the ascending gas bubbles, and downwards in the remaining emulsion phase), and completely ignores the presence of diffusion transport in the continuous bed phase. The one-concentration equation of convective diffusion formulated in [3] takes account of both diffusion and circulation transport, and here to calculate the latter we need detailed knowledge of the particle velocity distribution over time and system volume. This makes the model extremely awkward for practical use. The circulation-diffusion two-concentration mixing method proposed in [4] combines the good qualities of the diffusion and the circulation models. But even it is not free from the common defect generally inherent in the diffusion parabolic equations, that it does not take account of the inertia of the solid phase. As is well known [5], this leads to the paradox of infinitely large instantaneous velocity of particle motion. Therefore, in [5] particle mixing was described by the hyperbolic diffusion equations which, however, do not account for the circulation mixing mechanism.

Thus, neither of the above models includes all the basic features of the mixing process, and therefore does not satisfactorily describe the actual process over a wide range of variation of the experimental conditions.

In this paper the authors have tried to construct quite a universal model of the process, to describe both diffusion and circulation transport, and the inertia of the solid phase.

Three basic mechanisms have been identified for mixing of particles and bubbles in fluidized beds (Fig. 1):

- a) circulation (convective) transport of particles vertically;
- b) turbulent diffusion of particles at finite speed in the descending dense phase;
- c) horizontal exchange of particles between trails of gas bubbles and the descending dense phase.

The continuity equations for flux of labeled particles have the form

$$A \frac{\partial c_1}{\partial \tau} + A \frac{\partial w_i c_1}{\partial x_i} = \beta (c_2 - c_1),$$

$$B \frac{\partial c_2}{\partial \tau} + B \frac{\partial v_i c_2}{\partial x_i} = \beta (c_1 - c_2)^\dagger. \quad (1)$$

Here and below a repeated subscript indicates summation. Assuming, as in [4], that

$$v_i = u_1 \delta_{i1} + w'_i \ddagger, \quad v_i = -u_2 \delta_{i1}, \quad c_1 = C_1 + c'_1, \quad c_2 = C_2 + c'_2$$

and carrying out a standard time-average operation, we obtain

$$\begin{aligned} A \frac{\partial C_1}{\partial \tau} + Au_1 \frac{\partial C_1}{\partial x_1} &= -A \frac{\partial \langle w'_i c'_1 \rangle}{\partial x_i} + \beta (C_2 - C_1), \\ B \frac{\partial C_2}{\partial \tau} - Bu_2 \frac{\partial C_2}{\partial x_1} &= \beta (C_1 - C_2). \end{aligned} \quad (2)$$

We note that the Reynolds condition is satisfied here (see [4, 5]).

In order to bring system (2) to the form of the diffusion equations and also to account for particle inertia, we introduce the following analog of the Maxwell-Cattaniot relation:

$$\langle w'_i c'_1 \rangle = -D_{ij} \frac{\partial C_1}{\partial x_j} - \tau^* \left( \frac{\partial \langle w'_i c'_1 \rangle}{\partial \tau} + u_1 \frac{\partial \langle w'_i c'_1 \rangle}{\partial x_1} \right), \quad (3)$$

where  $\tau^*$  is the relaxation time of the concentration field  $c_1$ . The additional term  $-\tau^* u_1 \partial \langle w'_i c'_1 \rangle / \partial x_1$  (compared with the flux factor  $\langle w'_i c'_1 \rangle$ ) used previously, see, e.g., [5]) in Eq. (3) accounts for the presence of convective transport (with velocity  $u_1$ ) of the labeled mixture in the space of the descending continuous phase.

Combining Eqs. (2) and (3) we obtain

$$\begin{aligned} A \frac{\partial C_1}{\partial \tau} + u \frac{\partial C_1}{\partial x_1} + A\tau^* \frac{\partial^2 C_1}{\partial \tau^2} + 2u\tau^* \frac{\partial^2 C_1}{\partial \tau \partial x_1} &= \left( AD_{ij} - \frac{\tau^* u^2}{A} \delta_{i1} \delta_{1j} \right) \frac{\partial^2 C_1}{\partial x_i \partial x_j} + \beta (C_2 - C_1) \times \\ &\times \left( 1 + \tau^* \frac{\partial}{\partial \tau} + \tau^* u_1 \frac{\partial}{\partial x_1} \right); \quad B \frac{\partial C_2}{\partial \tau} - u \frac{\partial C_2}{\partial x_1} = \beta (C_1 - C_2). \end{aligned} \quad (4)$$

The equations of system (4) are a mathematical model for particle mixing in nonuniform fluidized beds. Taking account of the large difference in the volume heat capacities of the gas and the particles ( $\rho_f C_f : \rho_s C_s \sim 10^{-3}$ ), we may assume that all the heat in the system is transferred by the moving particles. Thus, Eq. (4) also describes the basic laws for internal heat transfer in the fluidized bed (in this case one must substitute:  $C_1 \rightarrow t_1$ ;  $C_2 \rightarrow t_2$ ;  $D_{ij} \rightarrow a_{ij}$ ;  $\beta \rightarrow \alpha$ ). One can also postulate that the condition  $D_{ij} = a_{ij}$  holds in nonuniform fluidized beds.

For  $\tau^* = 0$  system (4) describes the circulation-diffusion mixing model [4], and for  $\tau^* = 0$  and  $D_{ij} = 0$  it describes the Van Deemter circulation model [2]. Putting  $\tau^* = 0$ ,  $u_1 = u_2 = 0$ ,  $\beta = \infty$  ( $C_1 = C_2 = C$ ) in Eq. (4), we obtain the very simple diffusion model [1].

We now analyze the behavior of Eq. (4) at large time. Following the method of [2] we perform a Laplace transformation of Eq. (4) for the case  $C_1(0, x_1) = C_2(0, x_1) = 0$ ;  $\partial C_1(0, x_1) / \partial \tau = 0$ :

$$\begin{aligned} Ap\bar{C}_1 + u \frac{\partial \bar{C}_1}{\partial x_1} + A\tau^* p^2 \bar{C}_1 + 2u\tau^* p \frac{\partial \bar{C}_1}{\partial x_1} &= \\ = \left( AD_{ij} - \frac{\tau^* u^2}{A} \delta_{i1} \delta_{1j} \right) \frac{\partial^2 \bar{C}_1}{\partial x_i \partial x_j} + \beta (\bar{C}_2 - \bar{C}_1) \left( 1 + \tau^* p + \tau^* u_1 \frac{\partial}{\partial x_1} \right), \\ Bp\bar{C}_2 - u \frac{\partial \bar{C}_2}{\partial x_1} &= \beta (\bar{C}_1 - \bar{C}_2). \end{aligned} \quad (5)$$

†Strictly speaking, Eq. (1) is valid for the case when a small physical volume contains many bubbles. However, to a first approximation one can consider such a volume to be the so-called elementary cell of the bed — one bubble and the emulsion phase surrounding it. This is valid for stagnated layers, although this approach is widely used, in fact, even for free fluidized systems in writing the equations for the various two-phase models of the fluidized bed (see, e.g., [1, 2]).

‡The influence of horizontal particle transfer devices at the top of the bed and in the gas distribution device, which involves local details, can be accounted for in the velocity fluctuation  $w'_i$ .

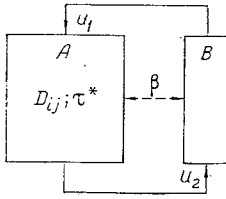


Fig. 1. Scheme of the two-phase model of mixing of particles and bubbles in a fluidized bed.

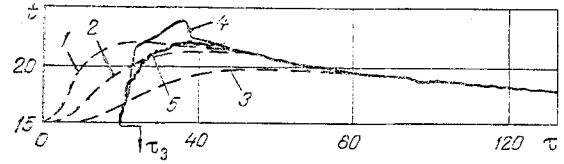


Fig. 2. Comparison of the calculated (1-4) and the experimental (5) temperature curves. The staggered beam bundle has  $S_V \times S_H = 60 \times 60$  mm;  $x_2/l = 0.85$ ;  $u_f = 131$  cm/sec;  $d = 0.63$  mm;  $t_0 = 15^\circ\text{C}$ ;  $t_c = 65^\circ\text{C}$ ; diffusion model: 1)  $a_h = 24.8$  cm<sup>2</sup>/sec; 2) 14.2; 3) 7.1 ( $\beta^* = 0.0068$  1/sec); diffusion model with finite particle velocity: 4)  $a_h = 12.8$  cm<sup>2</sup>/sec;  $\tau^* = 6.9$  sec ( $\beta^* = 0.0068$  1/sec).

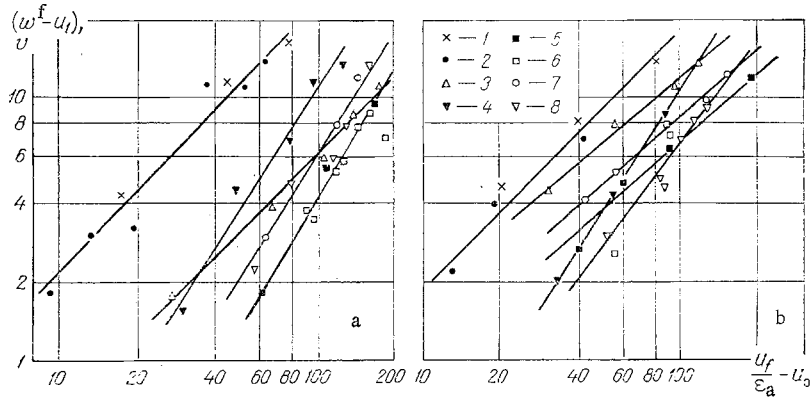


Fig. 3. Experimental data on velocities  $w^f - u_1$  and  $v$ : a) glass beads ( $d = 1.75$  mm); b) quartz sand ( $d = 0.63$  mm); 1, 2) free layer; 3, 4)  $S_V \times S_H = 60 \times 60$  mm ( $\epsilon_a = 0.80$ ); 5, 6)  $S_V \times S_H = 45 \times 45$  mm ( $\epsilon_a = 0.65$ ); 7, 8)  $S_V \times S_H = 60 \times 60$  mm ( $\epsilon_a = 0.80$ ). 1, 3, 5, 7) ( $w^f - u_1$ ); 2, 4, 6, 8)  $v$ ; 3-6) staggered bundle; 7, 8) corridor type; ( $w^f - u_1$ ),  $v$  in cm/sec;  $t$ ,  $^\circ\text{C}$ ;  $\tau$ , sec;  $u_f/\epsilon_a - u_0$ , cm/sec.

From the second equation of Eq. (5) we express  $\bar{C}_1$  in terms of  $\bar{C}_2$  and  $\partial \bar{C}_2 / \partial x_1$ , and substitute this into the first equation of the system (5). Retaining only terms linear in  $p$  (as  $\tau \rightarrow \infty$ ,  $p \rightarrow 0$  [6]), we obtain

$$(A + B) p \bar{C}_2 = \left( AD_{ij} + \frac{u^2}{\beta} \delta_{ij} \delta_{ij} \right) \frac{\partial^2 \bar{C}_2}{\partial x_i \partial x_j} - \left( AD_{ij} - \frac{\tau^* u^2}{A} \delta_{ij} \delta_{ij} \right) \frac{u}{\beta} \frac{\partial^2 \bar{C}_2}{\partial x_i \partial x_j \partial x_j}. \quad (6)$$

The equations for  $\bar{C}_1$  and for the transform of the mean concentration  $\bar{C} = \frac{A \bar{C}_1 + B \bar{C}_2}{A + B}$  are identical to Eq. (6).

Taking into account that the direction of the gas stream coincides with the axis  $0x_1$  we can regard the axes  $0x_1$ ;  $0x_2$ ;  $0x_3$  as the principal axes of the tensor  $D_{ij}$  [5]. Assuming this and going back to the original  $C$ , we represent Eq. (6) in the form

$$\frac{\partial C}{\partial \tau} = \left[ \frac{AD_{ii}}{A + B} + \frac{u^2 \delta_{ii}}{\beta(A + B)} \right] \frac{\partial^2 C}{\partial x_i^2} - \left[ \frac{AD_{ii}}{A + B} - \frac{\tau^* u^2 \delta_{ii}}{A(A + B)} \right] \frac{u}{\beta} \frac{\partial^2 C}{\partial x_i \partial x_i^2}. \quad (7)$$

Thus, in general, even for large  $\tau$ , system (4) does not transform into the very simple diffusion equation, but goes back to a third-order equation of the type of Eq. (7). Equation (7) reduces to a very simple parabolic diffusion equation

$$\frac{\partial C}{\partial \tau} = \left[ \frac{AD_{11}}{A+B} + \frac{u^2}{\beta(A+B)} \right] \frac{\partial^2 C}{\partial x_1^2} + \frac{AD_{22}}{A+B} \frac{\partial^2 C}{\partial x_2^2} + \frac{AD_{33}}{A+B} \frac{\partial^2 C}{\partial x_3^2} \quad (8)$$

with  $u/\beta H \ll 1$ .<sup>†</sup> The expression in the square brackets in Eq. (8) is that generally used in the [1] for the effective coefficient of vertical diffusion of particles  $K$ .<sup>‡</sup> One of the terms  $D_v = AD_{11}/(A+B)$  is the coefficient of vertical turbulent diffusion of particles; the second term  $K_a = u^2/\beta(A+B)$  is the coefficient of axial "Taylor" diffusion, found, as is known [8], in systems with a uniform field of axial velocities ( $u_1, u_2$ ) and transfer of material in the radial direction ( $\beta$ ). In circular and square beds it is permissible to take  $D_{22} = D_{33}$ . The expression  $AD_{22}/(A+B) = D_H$  is the effective coefficient of horizontal diffusion of particles.

It can be seen from Eq. (7) that the steady-state distribution of concentrations can be calculated from one of the two equations:

1) the vertical mixing:

$$K \frac{d^2 C}{dx_1^2} = \left[ \frac{AD_{11}}{A+B} - \frac{\tau^* u^2}{A(A+B)} \right] \frac{u}{\beta} \frac{d^3 C}{dx_1^3}, \quad (9)$$

2) the horizontal mixing:

$$\frac{d^2 C}{dx_2^2} = 0, \quad (10)$$

where the vertical concentration profile is determined, apart from coefficients of the third order of (9), like the diffusion flux, and can differ appreciably from linearity (horizontal mixing).

We now investigate the behavior of system (4) as the intensity of heat transfer between the phases varies.

a)  $\beta = 0$ , phases A and B are isolated. For the horizontal mixing case ( $C_1 = C_1(t, x_2)$ ;  $C_2 = C_2(t, x_2)$ ) Eq. (4) has the form

$$\frac{\partial C_1}{\partial \tau} + \tau^* \frac{\partial^2 C_1}{\partial \tau^2} = D_{22} \frac{\partial^2 C_1}{\partial x_2^2}; \quad \frac{\partial C_2}{\partial \tau} = 0. \quad (11)$$

The first equation in (11) describes diffusion with finite velocity  $v_0 = \sqrt{D_{22}/\tau^*}$  in the positive and negative directions of the  $0x_2$  axis. For vertical mixing ( $C_1 = C_1(t, x_1)$ ;  $C_2 = C_2(t, x_1)$ ) from Eq. (4) we obtain

$$\frac{\partial C_1}{\partial \tau} + u_1 \frac{\partial C_1}{\partial x_1} + \tau^* \frac{\partial^2 C_1}{\partial \tau^2} + 2u_1 \tau^* \frac{\partial^2 C_1}{\partial \tau \partial x_1} = (D_{11} - \tau^* u_1^2) \frac{\partial^2 C_1}{\partial x_1^2}; \quad \frac{\partial C_2}{\partial \tau} - u_2 \frac{\partial C_2}{\partial x_1} = 0. \quad (12)$$

In the coordinate system moving relative to the  $0x_1$  axis with velocity  $u_1$  Eq. (12) takes the form ( $x_1' = x_1 - u_1 \tau$ )

$$\frac{\partial C_1}{\partial \tau} + \tau^* \frac{\partial^2 C_1}{\partial \tau^2} = D_{11} \frac{\partial^2 C_1}{\partial x_1'^2}. \quad (12a)$$

Therefore, the first equation of (12) describes convective diffusion with finite velocity  $w_0^f = u_1 + \sqrt{D_{11}/\tau^*}$  in the positive  $0x_1$  axis direction; and with  $w_0^r = -u_1 + \sqrt{D_{11}/\tau^*}$  in the negative direction.

b)  $\beta = \infty$ , the phases A and B are physically indistinguishable ( $C_1 = C_2 = C$  and the system is single-phase). Expressing  $C_1$  from the second equation of (4) and substituting it into the first equation of (4) for the case  $\beta = \infty$ , we obtain

$$\frac{\partial C}{\partial \tau} + \tau^* \frac{\partial^2 C}{\partial \tau^2} = \frac{AD_{22}}{A+B} \frac{\partial^2 C}{\partial x_2^2} \quad (13)$$

for the horizontal mixing, and

$$\frac{\partial C}{\partial \tau} + \tau^* \frac{\partial^2 C}{\partial \tau^2} + u_1 \tau^* \frac{\partial^2 C}{\partial \tau \partial x_1} = \frac{AD_{11}}{A+B} \frac{\partial^2 C}{\partial x_1^2} \quad (14)$$

<sup>†</sup>This condition is fulfilled at least in high stagnated beds.

<sup>‡</sup>The quantity  $K = D_v + u^2/\beta(A+B)$  is not the coefficient of turbulent diffusion in the strict sense, and is therefore usually called the coefficient of vertical dispersion [7].

for the vertical mixing. The velocities and reverse waves determined by Eq. (13) are:  $v_{\infty} = \sqrt{\frac{AD_{22}}{(A+B)\tau^*}} = \sqrt{\frac{A}{A+B}} v_0$  ( $v_0$  is the wave velocity for  $\beta = 0$ ). The diffusion coefficient is equal to the effective horizontal diffusion coefficient  $D_h = AD_{22}/(A+B)$ .

The characteristics of Eq. (14) [9] have the form:

$$\begin{aligned} x_1 - \left[ \sqrt{\frac{AD_{11}}{(A+B)\tau^*} + \frac{1}{4}u_1^2} + \frac{1}{2}u_1 \right] \tau &= \text{const}_1, \\ x_1 + \left[ \sqrt{\frac{AD_{11}}{(A+B)\tau^*} + \frac{1}{4}u_1^2} - \frac{1}{2}u_1 \right] \tau &= \text{const}_2, \end{aligned} \quad (15)$$

and therefore, the velocity of the forward wave determined by Eq. (14) is  $\omega_{\infty}^f = \sqrt{AD_{11}/(A+B)\tau^* + u_1^2/4} + u_1/2$  and that of the reverse wave is  $\omega_{\infty}^r = \sqrt{AD_{11}/(A+B)\tau^* + u_1^2/4} - u_1/2$ . It is clear that the propagation velocity of the forward and reverse diffusion wave fronts horizontally for arbitrary  $\beta$  is  $v = \varphi(\beta)v_0$ , where  $\sqrt{A/(A+B)} \leq \varphi(\beta) \leq 1$ ;  $\varphi(0) = 1$ ;  $\varphi(\infty) = \sqrt{A/(A+B)}$ . The forward wave velocity  $w^f$  in the descending continuous phase for arbitrary  $\beta$  is  $w^f = \psi(\beta)w_0^f$ , where  $[\sqrt{AD_{11}/(A+B)\tau^* + u_1^2/4} + u_1/2]/(u_1 + \sqrt{D_{11}/\tau^*}) \leq \psi(\beta) \leq 1$ ;  $\psi(0) = 1$ ;  $\psi(\infty) = w_{\infty}^f/w_0^f$ . The reverse wave velocity  $w^r$  in this same phase varies in the range  $w_0^r$  to  $w_{\infty}^r$  with variation of  $\beta$  from 0 to  $\infty$ . The particle velocity in the bubble trail phase (the reverse wave velocity) is evidently equal to  $u_2$ , and thus, in the system with arbitrary  $\beta$  there are one forward wave and two reverse waves.† In actual fluidized systems  $A/(A+B)$  varies only very slightly:  $0.8 \leq A/(A+B) < 1$ . It can easily be seen that here  $\varphi(\beta)$  varies in the range  $0.9 < \varphi(\beta) \leq 1$ .

The function  $[\sqrt{AD_{11}/(A+B)\tau^* + u_1^2/4} + u_1/2]/(u_1 + \sqrt{D_{11}/\tau^*})$  depends weakly on  $u_1$ ,  $D_{11}/\tau^*$ , and  $A/(A+B)$ , and here  $\psi(\beta)$  varies in the range:  $0.77 < \psi(\beta) \leq 1$ . For the ratio  $w^f/v$  we obtain

$$\frac{w^f}{v} \cong \sqrt{\frac{D_{11}}{D_{22}} + u_1} \sqrt{\frac{\tau^*}{D_{22}}} \quad (16)$$

with an error not exceeding 16%. From Eq. (16), knowing  $\tau^*$ ,  $D_{22}$ ,  $u_1$ , and  $w^f/v$  we can evaluate  $D_{11}$ . The ratio between the coefficients  $D_{11}$  and  $D_{22}$  can be found from the following approximate equality:

$$\frac{D_{11}}{D_{22}} = \frac{D_v}{D_h} \cong \left( \frac{w^f - u_1}{v} \right)^2, \quad (16a)$$

which follows from Eq. (16).

An experimental determination of  $w^f$  and  $v$  was conducted in a rectangular facility of section  $40 \times 25$  cm. As disperse materials we used glass beads ( $d = 1.75$  mm;  $u_0 = 63$  cm/sec) and quartz sand ( $d = 0.63$  mm;  $u_0 = 20$  cm/sec). In determining  $w^f$  we used the method of an instantaneous planar heat source [10]. For a detailed description of the tests see [11]. The quantity  $w^f$  was found from the relation

$$w^f = l_x/\tau_d, \quad (17)$$

where  $l_x$  is the distance from the top of the bed (the place where the hot particles are introduced) to the point where the bed temperature changes; and  $\tau_d$  is the delay time of the response function (Fig. 2). An analogous method was used to determine  $v$  under horizontal mixing conditions. Here a heat pulse of finite width was created ( $l_0 = 6$  cm) by the method of [12] on the left-hand wall of the equipment. The velocity  $v$  was determined from:

$$v = (l_y - l_0)/\tau_d. \quad (18)$$

The measurement thermocouple was located at a distance  $l_y$  from the left-hand wall of the column.

In the work we studied both free beds and beds stagnated by means of horizontal tube bundles. Two types of staggered and straight-line bundles were used:  $S_v \times S_h = 45 \times 45$  mm,  $60 \times 60$  mm and  $S_v \times S_h = 60 \times 60$  mm.

†For  $w^r < 0$  in the system there are two forward waves ( $w^f$ ,  $-w^r$ ) and one reverse wave ( $-u_2$ ). It is evident that because of interphase transfer these three waves will be present in both phases.

Preliminary tests showed that  $w^f$  and  $v$  do not depend on  $H_0$ , and therefore the basic series of experiments was carried out in beds with  $H_0 = 25-27$  cm. The results obtained are shown in Fig. 3, from which, taking account of Eq. (16a) (the values of  $u_1$  were taken from [11]), it can be seen that in the free beds of both the disperse materials  $D_{11}$  is practically equal to  $D_{22}$ . An analogous situation occurs in the stagnated beds of glass beads in the straight line and staggered bundles ( $S_V \times S_h = 45 \times 45$  mm) (Fig. 3a). In the quartz sand beds  $D_{11} = (1-4)D_{22}$  in all the bundles. Here we can see a clear tendency for  $D_{11}$  and  $D_{22}$  to become close with increase in the filtration velocity (Fig. 3b). It is evident that the ratio of  $D_{11}$  and  $D_{22}$  is greatly influenced by processes of coalescence of bubbles and ejection of particles in the horizontal direction at the top of the bed and at the gas distribution device. As can be seen from Fig. 3, the contributions of these processes to the intensity of particle mixing in free beds is roughly the same, and they have a tendency to become close with increase of filtration velocity in stagnated beds.

Figure 2 shows a typical result of processing the experimental curves (5) according to the various models. Broken lines 1-3 show the system response functions to a heat pulse for the case of horizontal mixing of heated particles, calculated according to the solution [13] of the parabolic heat-conduction equation with boundary conditions corresponding to those created experimentally:

$$\frac{\partial t}{\partial \tau} = a_h \frac{\partial^2 t}{\partial x_2^2} - \beta^* (t - t_0), \quad (19)$$

$$t(0, x_2) = \begin{cases} t_c, & 0 \leq x_2 < l_0; \\ t_0, & l_0 < x_2 \leq l \end{cases}; \quad \frac{\partial t}{\partial x_2} = 0, \quad x_2 = 0; l,$$

where  $\beta^*$  is determined from the test response function from regular regime conditions [6] with  $\tau > \tau_{\max}$ . This parameter describes the heat flux from the bed to the tube bundle and to the air being filtered. It can be seen that the theoretical curves do not describe the actual heat-transfer process to the bed over the whole range of variation of time and, of course, do not contain  $\tau_d$ . The model constructed above allows this to be done. Using the analogy noted earlier between transport of labeled particles and heat in nonuniform fluidized beds, from system (4) we can obtain equations describing the horizontal internal heat transfer in the system:

$$A \frac{\partial t_1}{\partial \tau} + A\tau^* \frac{\partial^2 t_1}{\partial \tau^2} = Aa_{22} \frac{\partial^2 t_1}{\partial x_2^2} + [\alpha(t_2 - t_1) - A\beta^*(t_1 - t_0)] \times$$

$$\times \left( 1 + \tau^* \frac{\partial}{\partial \tau} \right); \quad B \frac{\partial t_2}{\partial \tau} = \alpha(t_1 - t_2) - B\beta^*(t_2 - t_0). \quad (20)$$

It was shown in [4] that the two-temperature system (20) with  $\tau^* = 0; \beta^* = 0; \alpha l^2 / a_{22} \geq 10$  converts to the one-temperature equation (19) (for  $\beta^* = 0$ ) with  $a_h = Aa_{22} / (A + B)$ . Therefore, for  $\alpha l^2 / a_{22} \geq 10$  (this usually holds in circular facilities [4]), Eq. (20) will take the form (eliminating one of the temperatures from Eq. (20) and putting  $t_1 = t_2 = t$  when  $\alpha \rightarrow \infty$ )

$$\frac{\partial t}{\partial \tau} + \tau^* \frac{\partial^2 t}{\partial \tau^2} = a_h \frac{\partial^2 t}{\partial x_2^2} - \beta^* (t - t_0) \left( 1 + \tau^* \frac{\partial}{\partial \tau} \right). \quad (21)$$

Allowing for the measured values  $\beta^* = 0.002-0.009$  1/sec and  $\tau^* = 1-5$  sec, Eq. (21) is simplified, and together with the required boundary conditions takes the form

$$\frac{\partial t}{\partial \tau} + \tau^* \frac{\partial^2 t}{\partial \tau^2} = a_h \frac{\partial^2 t}{\partial x_2^2} - \beta^* (t - t_0);$$

$$j = -a_h \frac{\partial t}{\partial x_2} - \tau^* \frac{\partial j}{\partial \tau} = 0, \quad x_2 = 0, l;$$

$$t(0, x_2) = \begin{cases} t_c, & 0 \leq x_2 < l_0; \\ t_0, & l_0 < x_2 \leq l \end{cases}; \quad \frac{\partial t(0, x_2)}{\partial \tau} = 0. \quad (22)$$

System (22) was used for numerical calculations of the temperature profiles, and here it was replaced by the equivalent system of equations

$$\frac{\partial t}{\partial \tau} = -\frac{\partial j}{\partial x_2} - \beta^* (t - t_0); \quad j = -a_h \frac{\partial t}{\partial x_2} - \tau^* \frac{\partial j}{\partial \tau} \quad (23)$$

and the boundary conditions

$$i(0, x_2) = \begin{cases} t_c, & 0 \leq x_2 < l_0; \\ t_0, & l_0 < x_2 \leq l; \end{cases} \quad j(0, x_2) = 0; \\ j(\tau, 0) = j(\tau, l) = 0.$$

Equations (23) were approximated by the fully conservative difference scheme [14] which was implemented numerically by a marching method [15] on a BESM-6 computer (the step sizes in the dimensionless coordinate  $x_2/l$  and in dimensionless time  $a_h\tau/l^2$  were 0.001 and 0.00001, respectively). The response function, calculated from Eq. (23), is also shown in Fig. 2 (4), from which it can clearly be seen that curve 4 describes the observed dependence over all the range of variation of  $\tau$  significantly better than do the functions 1-3 obtained from Eq. (19). This proves the importance of allowing for the inertia of the solid particles in describing transfer of particles and heat over the volume of a fluidized bed.

#### NOTATION

$a_{ij}$ , tensor for the bed diffusivity coefficients;  $a_h = Aa_{22} / (A+B)$ , effective coefficient of horizontal diffusivity of the bed;  $A = 1 - \varepsilon_v - \alpha_v \varepsilon_v$ , fractional volume of bed occupied by the descending continuum phase;  $B = \alpha_v \varepsilon_v$ , fractional volume of the bed occupied by bubble trails;  $C_s, C_f$ , heat capacity of the solid particles and the gas;  $c_1, c_2$ , mass of the labeled solid material arriving in unit volume of the emulsion phase in the descending continuum phase and in the bubble wakes, respectively;  $c'_1, c'_2$ , fluctuations in  $c_1$  and  $c_2$ ;  $C_1$  and  $C_2$ , mean values of  $c_1$  and  $c_2$ ;  $d$ , particle diameter;  $D_{ij}$ , tensor introduced in Eq. (3);  $D_h = AD_{22} / (A+B)$ , effective coefficient of

horizontal particle diffusion;  $H_0, H$ , initial and ambient bed height;  $j = Q / \rho C_s$ ;  $K = \frac{AD_{11}}{A+B} + \frac{u^3}{\beta(A+B)}$ , coefficient of vertical particle dispersion;  $p$ , Laplace parameter;  $Q$ , heat flux density;  $l_0, l$ , width of the heated chamber and of the equipment, respectively;  $S_v, S_h$ , vertical and horizontal pitch of the tubes;  $t_1$  and  $t_2$ , temperature of the solid particles in the emulsion phase and in the bubble trails, respectively;  $t = (At_1 + Bt_2) / (A+B)$ ;  $t_0, t_c$ , initial bed temperature and heated chamber temperature;  $u_1, u_2$ , velocity of the descending emulsion phase and of the bubble trails, respectively;  $Au_1 = Bu_2 = u$ , circulation velocity of the particles referred to the total section of the equipment;  $u_f$ , filtration velocity;  $u_0$ , velocity at the start of fluidization;  $w_i, v_i$ , velocities of the particles in the emulsion phase and in the bubble trails;  $w'_i$ , fluctuations in the quantity  $w_i$ ;  $x_1, x_2, x_3$ , vertical and horizontal coordinates;  $\alpha_v$ , fractional volume of the trail (referred to the gas bubble volume);  $\alpha^*$ , coefficient of heat transfer between the descending continuum phase and the bubble trails, referenced to unit volume of bed;  $\alpha = \alpha^* / \rho C_s$ ;  $\beta$ , volume of solid particles and gas between them (per unit time and unit bed volume) transferred between the descending continuum phase and the solid particles in the bubble trails;  $\beta^*$ , coefficient introduced into Eq. (19);  $\delta_{ij}$ , Kronecker delta;  $\varepsilon_v$ , concentration of bubbles in the bed;  $\varepsilon_a$ , porosity of the adapter;  $\rho_f, \rho_s$ , densities of the gas and the particles;  $\rho$ , density of the fluidized bed;  $\tau$ , time;  $\tau^*$ , relaxation time introduced into Eq. (3);  $\tau_d$ , delay time;  $\tau_{max}$ , time to reach the temperature maximum.

#### LITERATURE CITED

1. O. E. Potter, "Mixing," in: Fluidization [Russian translation], E. I. F. Davidson and D. Harrison (eds.), Khimiya, Moscow (1974), pp. 253-332.
2. J. J. Van Deemter, "The countercurrent flow model of a gas-solid fluidized bed," Proc. Int. Symp. Fluidization, Eindhoven (1967), pp. 334-347.
3. O. M. Todes, L. S. Sheinina, M. Z. Fainitskii, and M. A. Puzrin, "Two-parameter model of mixing of the solids in a fluidized bed," TOKhT, 14, No. 1, 139-144 (1980).
4. Yu. S. Teplitskii, "Circulation-diffusion model for mixing of solid particles in a fluidized bed," Izv. Akad. Nauk BSSR, Ser. Fiz. Energ. Nauk, No. 2, 119-126 (1981).
5. I. N. Taganov, Modeling of Mass and Energy Transfer Processes [Russian translation], Khimiya, Leningrad (1979).
6. A. V. Lykov, Heat Conduction [in Russian], Vysshaya Shkola, Moscow (1967).
7. M. É. Aérov and O. M. Todes, Hydraulic and Thermal Basis for Operation of Equipment with Stationary and Fluidized Granular Beds [in Russian], Khimiya, Leningrad (1968).
8. G. Taylor, "Dispersion of soluble matter in solvent flowing slowly through a tube," Proc. R. Soc. Ser. A, Math. Phys. Sci., 219, No. 1137, 186-203 (1953).
9. N. S. Koshlyakov, É. B. Gliner, and M. M. Smirnov, Equations in the Partial Derivatives of Mathematical Physics [in Russian], Vysshaya Shkola, Moscow (1970).
10. V. A. Borodulya and A. I. Tamarin, "Use of an instantaneous heat source to study mixing of particles in a fluidized bed," Inzh. -Fiz. Zh., No. 11, 101-104 (1962).

11. Yu. E. Livshits, A. I. Tamarin, and Yu. S. Teplitskii, "Mixing of large particles in a fluidized bed with tube bundles," *Izv. Akad. Nauk BSSR, Ser. Fiz. Energ. Nauk*, No. 4, 83-87 (1977).
12. V. M. Pakhaluev, "Investigation of the heat-transfer process in stagnated fluidized beds," Author's Abstract of Candidate's Dissertation, Technical Sciences, Sverdlovsk (1969).
13. Yu. S. Teplitskii, "Theory of unsteady methods of determining the effective diffusivity of a fluidized bed," *Izv. Akad. Nauk BSSR, Ser. Fiz. Energ. Nauk*, No. 3, 89-95 (1980).
14. A. A. Samarskii, *Theory of Difference Schemes* [in Russian], Nauka (1977).
15. A. A. Samarskii and E. S. Nikolaev, *Methods of Solving Mesh Equations* [in Russian], Nauka, Moscow (1978).

THE THERMODYNAMIC ANALYSIS OF MASS-TRANSFER MOTIVE FORCES IN THE COURSE OF CRYSTALLIZATION FROM SOLUTIONS

V. V. Kafarov, I. N. Dorokhov,  
and É. M. Kol'tsova

UDC 532.529.5 : 66.065.5

On the basis of taking the volume, mass, momentum, and energy of the surface phase into account, the structure of the motive forces of mass transfer to the phase interface (and from it into the carrier phase) in crystallization and solution is established. The correctness of the relations obtained is verified in two systems.

1. Structure of Dissipative Function of a Multiphase Medium in Which Crystallization Occurs

In accordance with the concepts outlined in [1], a multiphase medium is considered, where the first (carrier) medium is a solution, the  $r$ -th is crystals, of dimensions in the range  $(r - dr, r + dr)$ , and the surface phase is a  $\sigma$  phase (the  $\sigma$  phase is of volume  $V_\sigma$ , density  $\rho_\sigma^0$ , and temperature  $T_\sigma$ ). In the steady case, the intensity of mass transfer from the carrier phase into the  $\sigma$  phase and from the  $\sigma$  phase into the  $r$ -th phase is the same. In the most general case, however, the fluxes through the surface phase may be unequal; in other words

$$\rho_2^0 f \lambda dr \neq J_{1\sigma} f dr, \quad \rho_2^0 f \xi dr \neq J_{\sigma 1} f dr.$$

Let  $\eta = \lambda - \xi$ ,  $J = J_{1\sigma} - J_{\sigma 1}$ . By means of a discussion analogous to that outlined in [1], the following equations are obtained in differential form: mass conservation of the carrier phase

$$\frac{\partial \rho_1}{\partial t} + \text{div}(\rho_1 \mathbf{v}_1) = - \int_0^R J f dr, \tag{1}$$

mass conservation of the component in the carrier phase (in the interests of simplicity of exposition, it is assumed that only one component takes part in the phase transition)

$$\rho_1 \frac{d_1 c_{k1}}{dt} = (c_{k1} - 1) \int_0^R J f dr, \tag{2}$$

the balance of number of particles

$$\frac{\partial f}{\partial t} + \text{div}(f \mathbf{v}_2) + \frac{\partial f \eta}{\partial r} = 0, \tag{3}$$

---

Translated from *Inzhenerno-Fizicheskii Zhurnal*, Vol. 42, No. 2, pp. 260-266, February, 1982. Original article submitted April 13, 1981.